Membrane Interactions of Dynorphins[†,‡]

Jesper Lind, Astrid Gräslund, and Lena Mäler*

Department of Biochemistry and Biophysics, The Arrhenius Laboratories, Stockholm University, S-106 91 Stockholm, Sweden

Received June 16, 2006; Revised Manuscript Received September 20, 2006

ABSTRACT: The dynorphins are primarily endogenous ligands to the κ-opioid receptor, but a variety of non-opioid effects have also been observed, including direct effects on membranes. The peptides are rich in Arg residues, a characteristic feature of the cell-penetrating peptides. In this investigation, we have examined the interaction of the two peptides dynorphin A and dynorphin B with model membranes. A variety of NMR methods, as well as CD and fluorescence spectroscopy, have been used to characterize the structure of the two peptides and, more importantly, the position of the peptides in phospholipid bicelles. Both peptides interact to a large extent with both zwitterionic and partly negatively charged bicelles but are only marginally structured in either solvent. Dynorphin A was found to insert its N-terminus into the bilayer of the bicelle, while dynorphin B was found to reside on the surface of the bilayer. Despite the high degree of similarity in the sequence of the two peptides, it has previously been observed that dynorphin A has membrane perturbing effects and causes leakage of calcein from large unilamellar phospholipid vesicles while dynorphin B has no such effects. Our results provide a possible explanation for the difference in membrane perturbation.

Opioids constitute a general class of both natural and synthetic signal substances regulating the pain and reward system through interaction with any of the three κ-, δ-, and μ-opioid receptors in the central nervous system. This group contains among others morphine, heroin, endorphins, and dynorphins (*1*).

Dynorphins are all derivatives of prodynorphin (*2*), and they were first isolated during the late 1970s with the purpose of finding a way to regulate pain without the negative side effects of already known synthetic opioids (*3*, *4*). This powerful family of neuropeptides is mainly connected with pain regulation and analgesic effects (*5*, *6*). It has also been discovered that they are involved in a wide variety of physiological effects, such as influencing the motor system (*7*), causing hyperalgesia (*8*), and inducing apoptosis, among others (*9*, *10*).

Two central derivatives of prodynorphin are the Big dynorphin fractions dynorphin A (Dyn A,[1] YGGFLRRIRPKLKWDNQ) and dynorphin B (Dyn B, YGGFLRRQFKVVT) (*11*). These peptides are two of the most basic naturally occurring peptides in the body (*12*). Dyn A and Dyn B are primarily endogenous ligands to the κ-opioid receptor (KOR) but have also been shown to bind to the δ- and μ-opioid receptors (*13*, *14*). In addition to the versatility of these neuropeptides, experiments with the opioid receptor blocker naloxone have revealed that Dyn A causes non-opioid effects. These effects involve the NMDA receptor and may cause hyperalgesia, uncomfortable nociceptive behavior, and even paralysis (*10*, *11*, *15*).

Dyn A is rich in Arg and Lys residues, which is a characteristic feature of the so-called cell-penetrating peptides (CPPs). These peptides have the ability to internalize into cells with high efficiency, with low toxicity, and seemingly without any receptor while carrying large hydrophilic cargoes (*16*, *17*). Endocytotic mechanisms like raft-dependent macropinocytosis have been shown to be a dominant mechanism of internalization for CPPs like penetratin (*18*). However, direct membrane interactions are also important for CPPs either for endosomal escape or for direct cell membrane translocation which may also contribute to their internalization (*17*). Several models for the direct membrane translocation have been proposed, e.g., the carpet model (*19*) or the pore formation model (*20*). Although peptides possessing CPP characteristics most often adopt α-helix conformation when interacting with phospholipid bilayers, it has been shown that peptides with other structural propensities can act as CPPs (*21*).

A first step toward understanding the dynorphin−receptor interactions is to investigate the peptide−membrane interaction. A likely pathway for receptor binding has been suggested to begin with a preadsorption of the peptide to the membrane, followed by receptor interaction. This not only would simplify the interaction process between the signal substance and the receptor but also can induce structure and orientation of the peptide necessary for receptor interaction (*22*). Mechanisms for the initial interaction

[†] This work was supported by grants from the Swedish Research Council, The Carl Trygger Foundation, and the Magnus Bergvall Foundation.

[‡] The chemical shifts for dynorphin A and dynorphin B in H_2O, zwitterionic bicelles, and 20% negatively charged bicelles have been deposited with the BMRB as entries 7168 and 7169.

* To whom correspondence should be addressed. E-mail: lena.maler@dbb.su.se. Phone: +46 8 162448. Fax: +46 8 155597.

[1] Abbreviations: Dyn A, dynorphin A; Dyn B, dynorphin B; NMR, nuclear magnetic resonance; TOCSY, total correlation spectroscopy; NOESY, nuclear Overhauser enhancement spectroscopy; DHPC, 1,2-dihexanoyl-*sn*-glycero-3-phosphatidylcholine; DMPC, 1,2-dimyristoyl-*sn*-glycero-3-phosphatidylcholine; DMPG, 1,2-dimyristoyl-*sn*-glycero-3-phospho-1-glycerol.

10.1021/bi061199g CCC: $33.50
Published on Web 12/01/2006

between dynorphins and the lipid bilayer have been proposed but proved to be difficult to verify in a natural membrane environment (*23*, *24*). Several structural studies of neuropeptides in different membrane mimetic environments, such as helicogenic solvents, SDS, and DPC micelles, have been conducted (*25*−*28*), but due to nonrealistic membrane properties of such solvents, nothing is known about the molecular details of the interaction between the peptides and the membrane, e.g., the position in the membrane.

In this paper, the endogenous peptides Dyn A and Dyn B are studied in the presence of phospholipid bicelles. Bicelles are disk-shaped aggregates composed of long chain lipids arranging themselves as a bilayer surface with its rims covered by a detergent (*29*, *30*). The large curvature of small detergent micelles, which may induce unnatural peptide structure changes, and even loss of enzyme activity (*30*−*32*), is replaced with the phospholipid bilayer surface of the bicelle, which better describes the native environment of membrane-active peptides. The size of the bicelles as well as the net surface charge is easily regulated by adjusting the lipid/detergent ratio and by replacing neutral lipids with charged. Bicelles can be made sufficiently small ($q \leq 0.5$) to attain tumbling times suitable for liquid-state NMR spectroscopy while retaining the characteristic and useful disk shape (*33*). These properties make the bicelle comparable with vesicles as a membrane mimetic and enable solution-state NMR studies of the position of peptides in the membrane (*34*, *35*).

EXPERIMENTAL PROCEDURES

Sample Preparation. The peptides Dyn A and Dyn B were purchased from NeoMPS SA and used as received. The deuterated phospholipids 1,2-dimyristoyl-*sn*-glycero-3-phosphocholine (DMPC-d_{54}) and 1,2-dihexanoyl-*sn*-glycero-3-phosphocholine (DHPC-d_{22}), the spin-labeled 1-palmityl-2-steroyl-(5-DOXYL)-*sn*-glycero-3-phosphocholine, and undeuterated DMPC and DHPC were obtained from Avanti Polar Lipids. The deuterated 1,2-dimyristoyl-*sn*-glycero-3-[phospho-*rac*-(1-glycerol)] (DMPG-d_{54}) was obtained from Larodan AB.

Bicelles were produced by mixing DMPC thoroughly with H_2O until a slurry was formed. An aliquot of a 1 M stock solution of DHPC was added to obtain the desired q ratio (0.25−0.30), and the sample was vortexed and centrifuged until a clear liquid was obtained. The size of the bicelles is controlled by the ratio of the lipid and the detergent and can be estimated with the formula q = [long chain lipid]/[detergent] (*29*). Bicelles with negatively charged surfaces were produced by exchanging 10−30% of the zwitterionic DMPC for the negatively charged DMPG. The pH was adjusted to 5.7 with 50 mM phosphate buffer, and the peptide was added to the ready-made bicelles. In the NMR experiments, deuterated lipids (DHPC-d_{22}, DMPC-d_{54}, and DMPG-d_{54}) were used, and 10% D_2O was added for field frequency stability purposes.

NMR Spectroscopy. The NMR spectra were recorded on a Bruker Avance NMR spectrometer equipped with a cryoprobe operating at a ^{1}H frequency of 500 MHz and a Varian Inova NMR spectrometer equipped with a triple-resonance probe head operating at 600 MHz. All measurements were carried out at 37 °C. NOESY spectra (*36*) and TOCSY spectra (*37*) were recorded to investigate structural and interaction features of Dyn A and Dyn B (1 mM) in neutral and partly negatively charged bicelles (250 mM, q = 0.25−0.3). In the charged bicelles, 20% of the DMPC was replaced with DMPG. The NOESY spectra were recorded with mixing times of 100, 150, 300, and 800 ms, and the TOCSY spectra were recorded with mixing times of 65 and 30 ms; 2048 × 512 complex data points were collected using 48−64 scans. Water suppression was achieved either with the excitation sculpting sequence (*38*) or with Watergate (*39*). The spectra were processed and analyzed with FELIX (Accelrys, version 2001.1), and the processing included zero filling to 4096 × 2048 data points and apodizing the FIDs by multiplication with a 90°-shifted sine bell function prior to the Fourier transformation.

To determine the position of the peptides in bicelles, saturation transfer difference TOCSY (STD-TOCSY) (*40*) experiments were performed at 500 MHz with a sample containing 2 mM peptide in 250 mM undeuterated DHPC/DMPC bicelles (q = 0.30). Various DMPC ^{1}H resonances were saturated with a variable repetition of a 50 ms Gaussian pulse, leading to saturation times of 150, 300, 600, 800, and 1000 ms. The irradiations were performed at frequencies corresponding to the acyl chain methyl protons (0.86 ppm), the acyl chain methylene protons (1.24 ppm), or the glycerol 3-methylene protons (3.99 ppm). A reference spectrum was recorded by moving the carrier 30 ppm from the center of the spectrum (*41*). Intensity changes of H^N-H^α cross-peaks for Leu5, Lys11, Lys13, and Gln17 for DynA and Gly2, Val11, and Val12 for DynB were recorded and plotted as a function of the saturation time, T_{sat}. The excitation sculpting sequence was used for water suppression, 2048 × 200 complex data points were collected using 32 scans, and spectra were processed as described for the previously recorded TOCSY experiments.

As a complementary method for determining the position of the peptide, the effect of spin-labels on peak heights in a NMR spectrum was monitored by recording a two-dimensional (2D) TOCSY spectrum prior to and after adding spin-labeled lipids. Peak intensities in the H^N-H^α fingerprint region were measured in the 2D TOCSY spectrum of both DynA and DynB in either neutral or 20% negatively charged bicelles with a mixing time of 65 ms. A small amount (2.5 μL) of 0.1 M 1-palmitoyl-2-steroyl-(5-DOXYL)-*sn*-glycero-3-phosphocholine dissolved in methanol was added to a 500 μL sample to yield a final spin-label concentration of 0.5 mM, and a second TOCSY experiment was conducted. Increased line broadening of the peaks due to the paramagnetic relaxation enhancement is related to the distance to the lipid interface zone; thus, the relative position of the residues in relation to the membrane can be determined. Because of the mobility of the lipid hydrocarbon chains, it is, however, difficult to determine where in the membrane a certain part of a peptide is located, but the method gives a good approximation whether it is located inside or outside the membrane (*34*, *42*, *43*). The positioning studies were performed on the same samples that were used in the TOCSY and NOESY experiments.

Amide proton−deuterium exchange was measured at 600 MHz as a function of time for both peptides. A 1 mM sample of Dyn A and Dyn B in 250 mM neutral bicelles (q = 0.25) was prepared as described above, freeze-dried, dissolved in

650 μL of D_2O, and instantly placed in the spectrometer. A 4 h 2D TOCSY (2048 × 220 points, 16 scans) spectrum was then repeatedly recorded at 37 °C for both peptides.

To estimate the level of binding of the peptides to the bicelles, TOCSY spectra were recorded (at 500 mHz) with several different total lipid concentrations (150, 250, and 300 mM total phospholipid).

Circular Dichroism Spectroscopy. All CD spectra were recorded on a JASCO J-720 CD spectropolarimeter with a 0.01 mm cuvette at 37 °C. Spectra were recorded with 20 scans over the interval of 190−250 nm, with a bandwidth of 0.2 nm and a speed of 50 nm/min. Measurements were made for Dyn A (100 μM) and Dyn B (100 μM) in neutral bicelles (250 mM, $q = 0.30$) and 30% negatively charged bicelles (250 mM, $q = 0.30$) and a phosphate buffer solution (50 mM, pH 5.7).

Fluorescence Spectroscopy. All measurements were performed on a Perkin-Elmer LS 50B luminescence spectrometer with FL WINLAB. The experiments were conducted at room temperature with 4 mm × 10 mm cuvettes. Fluorescence excitation of Trp was at 280 nm, and the emission was detected over the interval of 275−400 nm. Fluorescence excitation of Tyr was at 272 nm, and emission was detected over the interval of 275−400 nm. Scans were recorded with a 4 nm bandwidth at a scan speed of 200 nm/min, and five scans were recorded and averaged for each sample. Measurements for Dyn A (containing one Trp residue) were conducted with a peptide concentration of 15 μM. Measurements for Dyn B (containing one Tyr residue) were performed with a peptide concentration of 100 μM. For both peptides, experiments were performed in neutral bicelles (200 mM, $q = 0.30$), 30% negatively charged bicelles (200 mM, $q = 0.30$), and a phosphate buffer solution (50 mM, pH 5.7), and the fluorescence was quenched with acrylamide at concentrations of 0, 4, and 40 mM. The quenching constants (K_{SV}) for each system were calculated through linear regression with the Stern−Volmer equation for a dynamic process (*44*):

$$\frac{F_0}{F} = 1 + K_{SV}[Q]$$

where F and F_0 are the fluorescence intensities in the presence and absence of the quencher, respectively, and [Q] is the concentration of acrylamide.

RESULTS

Assignment and Secondary Structure of the Peptides. Two-dimensional ^{1}H TOCSY and NOESY spectra were recorded for Dyn A and Dyn B in neutral bicelles, partly negatively charged bicelles, water, and phosphate buffer (pH 5.7). All backbone proton resonances of Dyn A with the exception for Tyr1 and Pro10 were assigned. All backbone resonances of Dyn B with the exception of Tyr1 were assigned in both bicelle solvents. Arg7, Lys10, and Thr13 in Dyn B were not assigned in a buffer/H_2O solution. The assignments have been deposited with the BioMagResBank as entries 7168 and 7169.

Only small variations in the chemical shifts could be observed between charged and zwitterionic bicelles for either of the peptides, although the increased charge of the lipid bilayer led to significant line broadening. The spectra of peptides in phosphate buffer and water were close to identical but differed greatly from the spectra in bicelles. Assignment of the bulk of the side chain resonances was made for Dyn A in neutral bicelles (84% of the side chain resonances), which enabled determination of 68 NOE constraints, 22 of which are inter-reside restraints (Figure 1). The major part of the detected NOEs involves N-terminal residues Gly3−Phe5 and also Arg7 and Ile8, for which α-helical H^N−H^N cross-peaks were observed; on the other hand, the C-terminus is much less represented and very few characteristic α-helix NOE cross-peaks could be found. These data are consistent with previous results, indicating limited secondary structure.

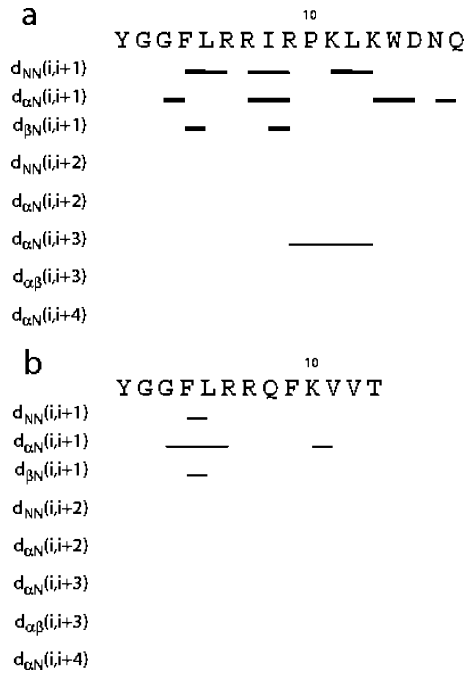

FIGURE 1: Summary of helical NOEs observed for Dyn A (a) and Dyn B (b) in neutral bicelles. The NOE connectivities were obtained from a 500 MHz NOESY spectrum recorded with a mixing time of 100 ms at 37 °C. The image was prepared with DYANA (version 1.5).

Very few (and weak) inter-residue NOEs were found for Dyn B (Figure 1), which shows that, despite the sequence similarity between the two peptides, Dyn B is even less structured in bicelles. As for Dyn A, however, the chemical shifts are very different in bicelles compared to those in water or buffer, indicating a membrane interaction of Dyn B.

Secondary chemical shifts for H^α protons were calculated according to the method of Wishart and Sykes (*45*). In the figure containing H^α secondary chemical shift for Dyn A in bicelles (Figure 2a,b), a propensity for the N-terminal residues to adopt a helix structure can be observed, a tendency that becomes stronger with charge and which is not present in buffer (Figure 2c). This suggests that the N-terminal residues may be more deeply involved in the interaction with the bilayer than the rest of the peptide, and this induces a propensity for structure in the first five residues of the peptide. Dyn B in bicelles shows no tendency to adopt any defined structure from interacting with bicelles, although the resonances clearly differ from the typical random coil shifts measured in a phosphate buffer solution (Figure 2d,e). The H^α secondary chemical shifts in buffer solution are very close to random coil values for both peptides.

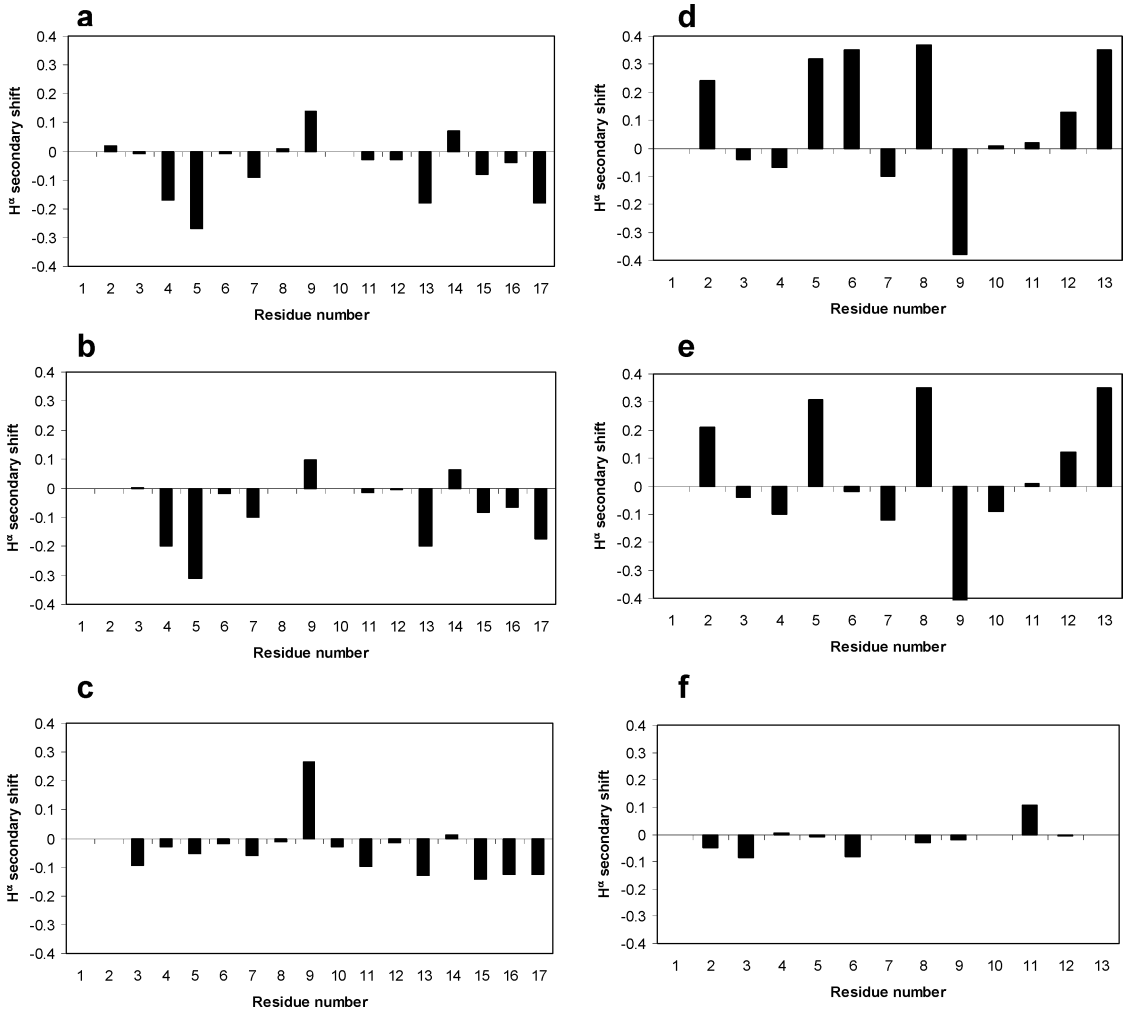

FIGURE 2: Secondary H^{α} chemical shifts for DynA and DynB. (a) Secondary chemical shifts for DynA in 250 mM DHPC/DMPC bicelles ($q = 0.25$). (b) DynA in 250 mM (20%) acidic bicelles ($q = 0.25$; [DMPG]/[DMPC] = 0.2). (c) DynA in 50 mM phosphate buffer. (d) DynB in 250 mM DHPC/DMPC bicelles ($q = 0.25$). (e) DynB in 250 mM acidic bicelles (20%) ($q = 0.25$; [DMPG]/[DMPC] = 0.2). (f) DynB in 50 mM phosphate buffer.

To investigate peptide−bicelle binding, the effects of varying the total lipid concentration were examined. TOCSY spectra were recorded for the peptides dissolved in a neutral $q = 0.25$ bicelle solution with total lipid concentrations of 150, 250, and 300 mM. The chemical shifts of the majority of the H^N and H^{α} resonances remain totally unaffected by the change in lipid concentration, and the maximum change is less than 0.05 ppm. This is in contrast to the large differences in chemical shifts seen for the peptides in bicelle solutions compared to buffer solutions. Since varying the lipid concentration does not affect the spectrum of the peptides, the conclusion can be drawn that they are mostly bound to the bicelle, with no evidence of any significant exchange between the free and bound peptide.

Position of the Peptides in Bicelles. Differences between measured H^N chemical shifts and random coil values can reveal information about the environment of the residue, as well as hydrogen bonding within helical structures, or to water molecules (*45*, *46*). Typically, chemical shifts for H^N resonances in residues in a hydrophobic environment are shifted to higher values relative to the average, while they are shifted toward lower values in a polar environment. Here we see that the H^N shift differences for resonances in the N-terminal residues (Gly2−Phe4) in Dyn A differ significantly from the rest of the peptide, indicating an interaction with the hydrophobic interior of the bicelle (Figure 3). The same result is seen in either neutral or partly negatively charged bicelles. This indicates that this part of the peptide (the N-terminus) interacts with the bicelle in a different way than the rest of the peptide. For Dyn B, no specific tendencies in chemical shifts related to any part of the peptide could be observed. Again, similar observations are made in both types of bicelle solution.

To further investigate the interaction between the two peptides and the bicelles, phospholipids labeled with a paramagnetic doxyl group in position 5 in the acyl chain were added to both neutral and partly negatively charged bicelles, and the effect on peptide H^N-H^{α} cross-peaks was monitored (Figure 4). First, we see that for both peptides, the paramagnetic probe has a very similar effect on the intensities in the two bicelles, indicating that the membrane interaction is independent of surface charge. For Dyn A, the results show that the paramagnetic spin-label affects the N-terminus the most, which indicates that this part of the peptide is spatially closest to the paramagnetic label, i.e., the acyl chains of the lipids. The C-terminus is not affected and is thus more likely positioned within the headgroup region, or outside of the bicelle.

For Dyn B, the results are again less clear and a somewhat different picture is seen. Every three or four residues in the

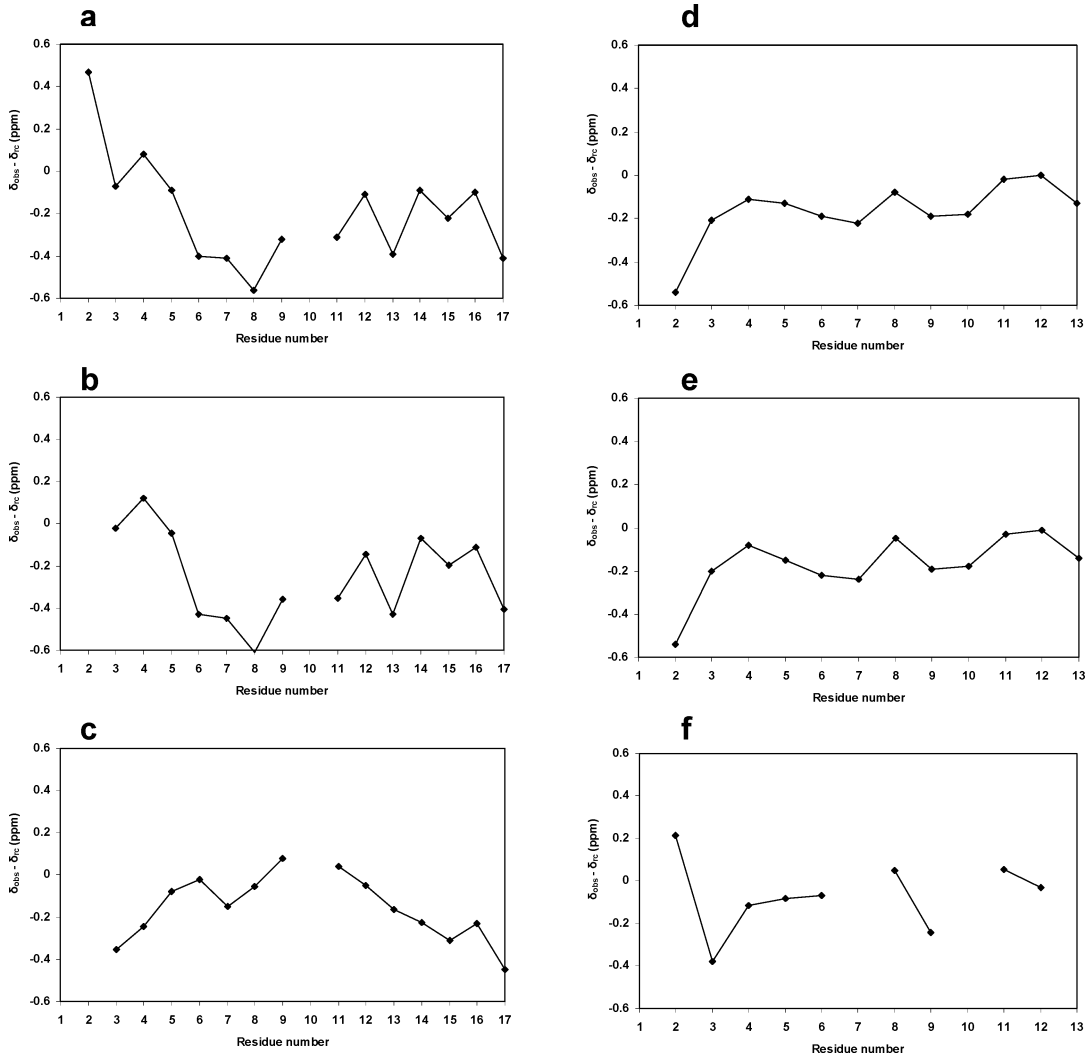

FIGURE 3: Differences between observed and random coil H^N chemical shifts for Dyn A and Dyn B. (a) Differences in chemical shifts for DynA in 250 mM DHPC/DMPC bicelles ($q = 0.25$). (b) DynA in 250 mM acidic bicelles (20%) ($q = 0.25$; [DMPG]/[DMPC] = 0.2). (c) DynA in 50 mM phosphate buffer. (d) DynB in 250 mM DHPC/250 mM DMPC bicelles ($q = 0.25$). (e) DynB in 250 mM acidic bicelles (20%) ($q = 0.25$; [DMPG]/[DMPC] = 0.2). (f) DynB in 50 mM phosphate buffer.

sequence are greatly affected by the 5-doxyl group (residues Phe4, Arg6, and Phe9). The effect of the spin-label indicates that the peptide most likely associates with both bicelle surfaces in a somewhat loose way.

We examined the interaction between the peptides and the bicelle in more detail by conducting saturation transfer difference (STD) experiments. The changes in intensity [i.e., $(I_0 - I_{sat})/I_0$] of H^N-H^α cross-peaks of selected residues were measured and plotted as a function of saturation time (Figures 5 and 6) for various DMPC resonances. The methyl group signal for DMPC was seen to overlap with that of C^δ methyl protons in Ile8 in Dyn A. Furthermore, the glycerol signal overlaps partly with that of one of the H^α protons in Gly3. Therefore, we did not investigate the effect on these and sequentially close residues. One should also point out that the signals corresponding to the different sites in DMPC chosen for irradiation are not equivalent with regard to intensity, especially the signal corresponding to the bulk of the acyl chain protons. Furthermore, longer mixing times will render greater spin diffusion effects which makes it difficult to estimate actual distances, but it is still possible to compare relative distances between a residue and different parts of the lipid.

In Figure 5, the cross-relaxation buildup curves obtained from intensity changes in H^N-H^α cross-peaks in TOCSY spectra for Leu5, Lys11, Lys13, and Gln17 of Dyn A are plotted as a function of the irradiation time of the frequencies corresponding to the proton resonances in DMPC indicated in Figure 5e (terminal acyl chain methyl, acyl chain methylene, and glycerol methylene groups). Starting with Leu5 (Figure 5a), we see that the strongest effect on the intensity for this proton is from irradiating the methylene protons, while irradiating the glycerol and methyl group protons has a weaker effect. We interpret this result as evidence that residues close to the N-terminus insert into the bilayer.

For Lys11, a similar trend is observed, with the strongest cross-relaxation being from the methylene and methyl group protons. One should keep in mind that the resonance corresponding to the acyl chain methyl group overlaps with that of the C^δ protons in Ile8, which may be spatially close to Lys11, leading to an overestimate of the degree of cross-

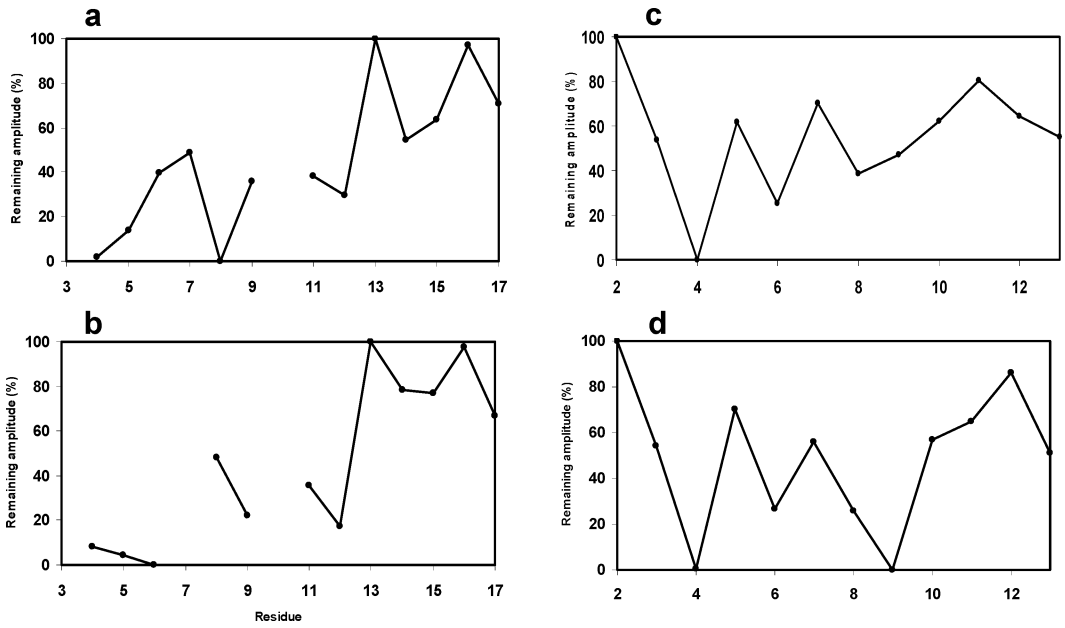

FIGURE 4: Remaining intensity of H^N-H^α cross-peaks in a TOCSY spectrum (t_{mix} = 65 ms) after the addition of 0.75 mM 1-palmityl-2-steroyl-(5-DOXYL)-*sn*-glycero-3-phosphocholine. (a) DynA in 250 mM DHPC/DMPC bicelles (q = 0.25). (b) DynA in 250 mM acidic bicelles (10%) (q = 0.25; [DMPG]/[DMPC] = 0.1). (c) DynB in 250 mM neutral bicelles (q = 0.25). (d) DynB in 250 mM acidic bicelles (20%) (q = 0.25; [DMPG]/[DMPC] = 0.2).

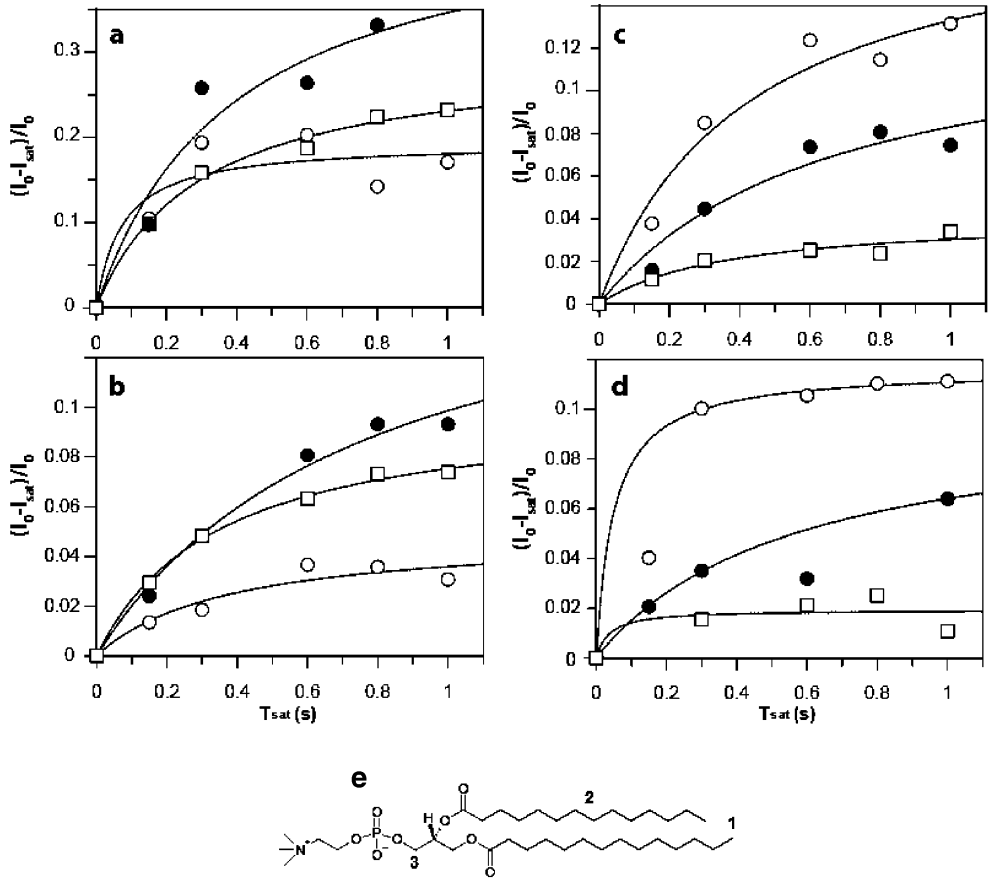

FIGURE 5: Observed STD effect of selected H^N-H^α cross-peaks in Dyn A calculated as $(I_0 - I_{sat})/I_0$ during selective irradiation of various DMPC resonances: (a) Leu5, (b) Lys11, (c) Lys13, and (d) Gln17. The saturated protons in DMPC are indicated by number (1−3) in the structure displayed in panel e. Experimental results from irradiation of the acyl chain methyl protons (point 1) are marked with squares, from irradiation of acyl chain methylene protons (point 2) with filled circles, and from irradiation of the glycerol methylene protons (point 3) with empty circles.

relaxation from the lipid. Turning to the results for Lys13 and Gln17, we find that the most pronounced effect is from irradiating the glycerol protons, while no significant cross-relaxation between the acyl chain methyl group protons and

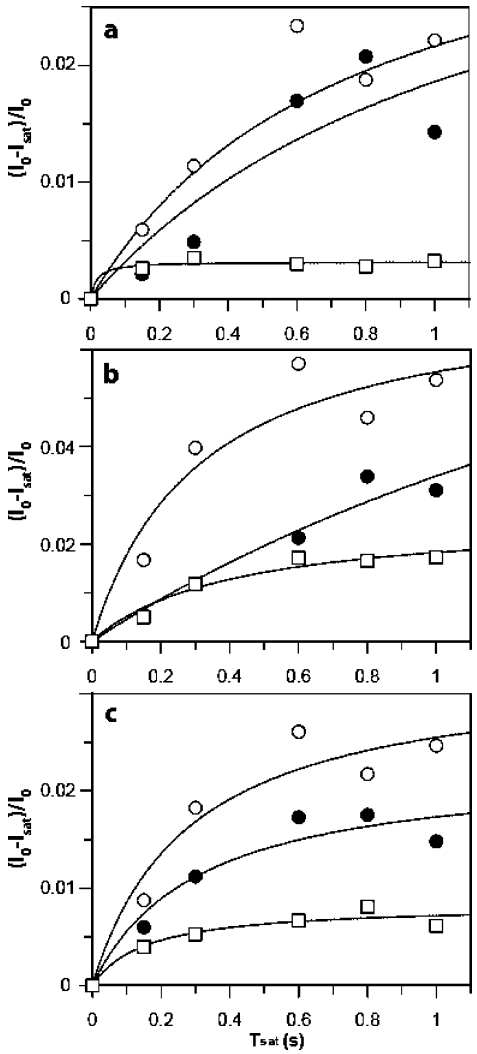

FIGURE 6: Observed STD effect of selected H^N-H^α cross-peaks in Dyn B calculated as $(I_0 - I_{sat})/I_0$ during selective irradiation of various DMPC resonances:(a) Gly2, (b) Val11, and (c) Val12. The saturated protons in DMPC are indicated by number (1−3) in the structure displayed in Figure 5e. Experimental results from irradiation of the acyl chain methyl protons (point 1) are marked with squares, from irradiation of acyl chain methylene protons (point 2) with filled circles, and from irradiation of the glycerol methylene protons (point 3) with empty circles.

these residues is observed. This shows that the residues closer to the C-terminus preferentially interact with the headgroup region of the bilayer.

For Dyn B, H^N-H^α cross-peaks for three residues, Gly2, Val11, and Val12, were analyzed in the same way (Figure 6). In all cases, we found that the strongest cross-relaxation was seen to be due to irradiating the glycerol protons. For Gly2, an appreciable amount of cross-relaxation is also observed when irradiating the methylene protons. No significant effect was observed from irradiating the acyl chain methyl group protons on any of the residues. This shows that the entire Dyn B peptide has a position close to the headgroup region of the bicelle bilayer.

The cross-relaxation results were confirmed by analyzing cross-peaks in a NOESY spectrum with a long mixing time (800 ms). For Dyn A, a relatively large cross-peak between the methylene protons in the lipid and Phe4 was observed, while the corresponding cross-peak between the glycerol protons in the lipid and Phe4 was very weak. The opposite

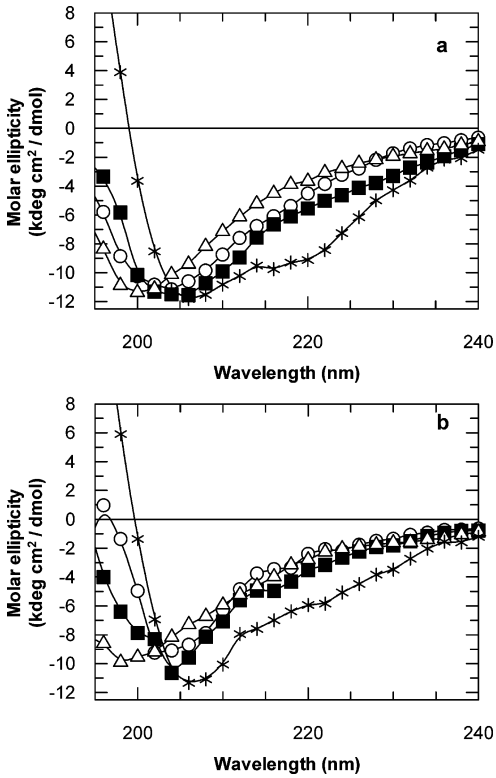

FIGURE 7: CD spectra for Dyn A and Dyn B in different solvents, recorded at 37 °C. (a) CD spectra for 100 μM Dyn A in 250 mM DHPC/DMPC bicelles (q = 0.30) (○), 250 mM acidic bicelles (30%) (q = 0.30; [DMPG]/[DMPC] = 0.3) (■), 50 mM phosphate buffer (pH 5.6) (△), and 99% TFE (∗). (b) CD spectra for DynB in 200 mM DHPC/DMPC bicelles (q = 0.30) (○), 250 mM acidic bicelles (30%) (q = 0.30; [DMPG]/[DMPC] = 0.3) (■), 50 mM phosphate buffer (pH 5.6) (△), and 99% TFE (∗).

was observed for N-terminal residue Asn16. For Dyn B, cross-peaks between the lipid and the peptide were generally weak, and only weak cross-peaks between the glycerol protons and the peptide could be observed.

H^NHydrogen−Deuterium Exchange. 2D TOCSY (recorded over 4 h) experiments were conducted for each of the peptides in a neutral bicelle solution. All H^N protons were exchanged for deuterium during the first experiment; thus, no peaks could be seen in the spectrum for either Dyn A or Dyn B. This is much faster than previous studies with more deeply buried cell-penetrating peptides as well as more transmembrane peptides (*47*, *48*) and agrees with the conclusion that the peptides are bound to the bicelle surface and exposed to the solvent (*49*).

Circular Dichroism Spectroscopy. CD measurements give an overview of the secondary structure of a peptide induced by its surroundings. Spectra were recorded for Dyn A and Dyn B in phosphate buffer solution, neutral bicelles, 30% negatively charged bicelles, and 99% TFE, and the results are presented in Figure 7.

The CD spectra of both Dyn A and Dyn B in buffer solution reveal a typical random coil structure and do not show any dominating secondary structure (Figure 7a-i,b-i) (*50*). The spectra for the peptides dissolved in neutral and charged bicelles show to some extent shifts of the spectra toward an α-helix appearance, but the overall conclusion is still that both peptides have largely unordered conformations. However, certain differences in the appearance of the spectra for both peptides can be observed, especially in the region

Table 1: Tryptophan and Tyrosine Fluorescence for Dyn A and Dyn B

	Dyn A (Trp as the fluorophore)		Dyn B (Tyr as the fluorophore)	
	λ_{peak} (nm)	K_{SV} (M^{-1})	λ_{peak} (nm)	K_{SV} (M^{-1})
phosphate buffer	352	30.7	302	29.0
neutral bicelles	348	13.5	306	13.9
30% negatively charged bicelles	347	11.8	306	15.9

around 200 nm. This is in good agreement with previous studies of the dynorphins in phospholipid vesicles and shows that the two peptides interact with both neutral and negatively charged bicelles (*51*).

Organic solvents such as TFE can be used to elucidate the propensity of a peptide to undergo a structural conversion. Using 99% TFE as solvent results in a significant increase in α-helix structure content for Dyn A (Figure 7a). The same trend is observed also for Dyn B in 99% TFE (Figure 7b), but in agreement with the results with the other solvents, the induced structure content is less than that for Dyn A.

Fluorescence Spectroscopy. To determine if the two peptides interact with the bicelles in a manner similar to what has previously been observed in liposomes (*51*, *52*), the intrinsic fluorescence of Trp and Tyr was measured for both peptides in neutral and 30% negatively charged bicelles, as well as in the buffer environment. Dyn A contains a Trp residue at position 14, while Dyn B lacks Trp but has a Tyr as its first residue. The quencher acrylamide acts as a neutral hydrophilic quencher (*53*), and the fluorescence quenching as a function of quencher concentration can be monitored via the Stern−Volmer equation (*45*).

The Trp residue in Dyn A has a peak emission wavelength of 352 nm and a Stern−Volmer quenching constant of 30 M^{-1} in buffer solution, which are close to the values of free Trp in water (354 nm and 35 M^{-1}, respectively) (*45*, *53*). A Trp residue completely situated in a hydrophobic environment has an emission maximum around 320 nm; hence, we conclude that in this case the Trp is not deeply buried within the bicelle. The presence of either neutral or partly negatively charged bicelles decreases the quenching constant by a factor of 2 (Table 1). This is in agreement with the observation that varying the lipid composition and concentration does not influence the proton chemical shifts and indicates that the peptide interacts with both types of bicelles in a similar manner. The results are in good agreement with what has previously been observed in phospholipid vesicles (*51*).

The same reduction (a factor of ∼2) in the quenching constant is seen for Tyr1 in Dyn B when it is placed in either bicelle solvent (Table 1), indicating that the peptide interacts with both neutral and partly negatively charged bicelles.

DISCUSSION

The dynorphin peptides have previously been shown to interact with phospholipid vesicles, resulting in only minor secondary structure changes (*51*). Despite the fact that the first seven residues of Dyn A and Dyorphin B are identical, a remarkable difference in membrane perturbation has been observed (*52*). Dyn A has been shown to induce a considerable amount of leakage in large unilamellar phospholipid vesicles, while Dyn B induces virtually no leakage at all. The difference between the two must be related to subtle differences in membrane interactions.

In this study, we have examined the differences in the membrane interaction of the two peptides and bicelles. The saturation transfer difference (STD) experiment provides a very elegant opportunity to determine the surroundings of single residues without disturbing the system with additives between measurements. Together with methods such as analysis of H^N secondary shifts and additions of spin-labeled lipids, a very consistent picture of how the peptides are positioned in a phospholipid bilayer can be made.

The combined results from all methods support the conclusion that Dyn A is bound to the surface of the bilayer with the N-terminal residues inserted into the hydrophobic bilayer region and the C-terminal residues more loosely attached to the surface. In addition, the amide proton exchange results indicate a position of the peptide that makes it available for the solvent and not buried in the membrane. This is in excellent agreement with solid-state NMR results, which showed that Dyn A inserts the first five residues into the membrane (*54*). In their study, however, they observed a more pronounced helical character for this part of the peptide than what is observed here. Earlier investigations of Dyn A in micelles (*29*) and of Dyn A (*1*−*13*) in lipid bilayers (*55*) also indicated a helical N-terminus, but the location of the peptide in the membrane medium differed somewhat.

Dyn B also binds to the bilayer, as evidenced from CD and fluorescence experiments, which affects its surroundings resulting in chemical shifts different from those observed in water or buffer, but it does not insert any parts into the lipids. None of the results presented here (chemical shifts, paramagnetic broadening, or STD results) indicate that the N-terminus is different from the rest of the peptide, which was seen for Dyn A. The results can be interpreted as a more parallel orientation throughout the peptide in relation to the bilayer. Very few interresidue NOEs were observed for this peptide, indicating even less structure than what is seen for Dyn A. This lower structural propensity may be the cause for the difference in orientation between the peptides and may partly explain previous observations that Dyn A is capable of causing leakage in phospholipid vesicles but Dyn B is not (*52*). It is striking that the two peptides interact and affect the membrane in such different ways, even though the first seven residues of these short peptides are identical. The major difference in sequence is the occurrence of five positively charged residues in Dyn A, while Dyn B only has three (*51*, *52*). The net charge of the peptides is, however, not that different (+4 for Dyn A vs +3 for Dyn B). The extent of the interaction with the membrane, however, does not seem to be dominated by charges, since virtually no differences are observed for either peptide in the two different types of bicelles. The only significant difference that can be detected is the increased line broadening in the NMR spectra in partly negatively charged bicelles, which has previously been explained with the stronger electrostatic interaction restraining the mobility of charged peptides within the bilayer and thus affecting the relaxation (*49*).

In conclusion, the results presented here show that Dyn A and Dyn B interact with phospholipid membranes. Only weak secondary structures are induced in the peptides despite the strong interaction with the bicelles. In addition, our results provide further understanding of the differences between the

cellular effects of Dyn A and Dyn B. The deeper insertion of the N-terminus of Dyn A into a membrane may be linked to its internalization into cells and its non-opioid properties which are significantly different from those of Dyn B (*10*).

REFERENCES

1. Stimmel, B., and Kreek, M. J. (2000) Neurobiology of Addictive Behaviours and its Relationship to Methadone Maintenance, *Mt. Sinai J. Med. 67*, 5−6.
2. Hauser, K. F., Aldrich, J. V., Anderson, K. J., Bakalkin, G., Christie, M., Hall, E., Knapp, P., Scheff, S., Singh, I., Vissel, B., Woods, A., Yakovleva, T., and Shippenberg, T. (2005) Pathobiology of Dynorphins in Trauma and Disease, *Front. Biosci. 10*, 216−235.
3. Goldstein, A., Tachibana, S., Lowney, L., Hunkapiller, M., and Hood, L. (1979) Dynorphin-(1−13), an Extraordinarily Potent Opioid Peptide, *Proc. Natl. Acad. Sci. U.S.A. 76*, 6666−6670.
4. Chavkin, C., James, I. F., and Goldstein, A. (1982) Dynorphin is a Specific Endogenous Ligand of the κ Opioid Receptor, *Science 215*, 413−415.
5. Han, J. S., and Xie, C. W. (1984) Dynorphin: Potent Analgesic Effect in Spinal Cord of the Rat, *Sci. Sin. 27*, 169−177.
6. Wen, H. L., Mehal, Z. D., Ong, B. H., and Ho, W. K. (1987) Treatment of Pain in Cancer Patients by Intrathecal Administration of Dynorphin, *Peptides 8*, 191−193.
7. Walker, J. M., Moises, H. C., Coy, D. H., Baldrighi, G., and Akil, H. (1982) Nonopiate Effects of Dynorphin and Des-Tyr-Dynorphin, *Science 218*, 1136−1139.
8. Trujillo, K., and Akil, H. (1991) Inhibition of Morphine Tolerance and Dependence by NMDA Receptor Antagonist MK-801, *Science 251*, 85−87.
9. Smith, A., and Lee, N. (1988) Pharmacology of Dynorphin, *Annu. Rev. Pharmacol. Toxicol. 28*, 123−140.
10. Tan-No, K., Cebers, G., Yakovleva, T., Goh, B., Gileva, I., Reznikov, K., Aguilar-Santelises, M., Hauser, K., Terenius, L., and Bakalkin, G. (2001) Cytotoxic Effects of Dynorphins through Nonopioid Intracellular Mechanisms, *Exp. Cell Res. 269*, 54−63.
11. Tan-No, K., Esashi, A., Nakagawasai, O., Niijima, F., Tadano, T., Sakurada, C., Sakurada, T., Bakalkin, G., Terenius, L., and Kisara, K. (2002) Intrathecally Administered Big Dynorphin, a Prodynorphin-Derived Peptide, Produces Nociceptive Behavior through an N-Methyl-D-Aspartate Receptor Mechanism, *Brain Res. 952*, 7−14.
12. Bakalkin, G. Y., Rakhmaninova, A. B., Akparov, V. K., Volodin, A. A., Ovchinnikov, V. V., and Sarkisyan, R. A. (1991) Amino Acid Sequence Pattern in the Regulatory Peptides, *Int. J. Pept. Protein Res. 38*, 505−510.
13. Höllt, V. (1986) Opioid Peptide Processing and Receptor Selectivity, *Annu. Rev. Pharmacol. Toxicol. 26*, 59−77.
14. Caudle, R. M., and Mannes, A. J. (2000) Dynorphin: Friend of Foe? *Pain 87*, 235−239.
15. Wollemann, M., and Benyhe, S. (2004) Non-Opioid Actions of Opioid Peptides, *Life Sci. 75*, 257−270.
16. Deshayes, S., Morris, M. C., Divita, G., and Heitz, F. (2005) Cell-Penetrating Peptides: Tools for Intracellular Delivery of Therapeutics, *Cell. Mol. Life Sci. 62*, 1839−1849.
17. Magzoub, M., and Gräslund, A. (2004) Cell-Penetrating Peptides: From Inception to Application, *Q. Rev. Biophys. 37*, 147−195.
18. Wadia, J. S., Stan, R. V., and Dowdy, S. F. (2004) Transducible TAT-HA Fusogenic Peptide Enhances Escape of TAT-Fusion Proteins After Lipid Raft Macropinocytosis, *Nat. Med. 10*, 310−315.
19. Pouny, Y., Rapaport, D., Mor, A., Nicholas, P., and Shai, Y. (1992) Interaction of Antimicrobial Dermaseptin and its Fluorescently Labeled Analogues with Phospholipid Membranes, *Biochemistry 31*, 12416−12423.
20. Matsuzaki, K., Murase, O., Fujii, N., and Miyajima, K. (1996) An Antimicrobial Peptide, Magainin 2, Induced Rapid Flip-Flop of Phospholipids Coupled with Pore Formation and Peptide Translocation, *Biochemistry 35*, 11361−11368.
21. Magzoub, M., Eriksson, L. E. G., and Gräslund, A. (2002) Conformational States of the Cell-Penetrating Peptide Penetratin when Interacting with Phospholipid Vesicles: Effects of Surface Charge and Peptide Concentration, *Biochim. Biophys. Acta 1563*, 53−63.
22. Moroder, L., Romano, R., Guba, W., Mierke, D. F., Kessler, H., Delporte, C., Winand, J., and Christophe, J. (1993) New Evidence for a Membrane-Bound Pathway in Hormone Receptor Binding, *Biochemistry 32*, 13551−13559.
23. Schwyzer, R. (1995) In search of the 'Bio-active conformation': It is induced by the target cell membrane? *J. Mol. Recognit. 8*, 3−8.
24. Schwyzer, R. (1991) Peptide-Membrane Interactions and a New Principle in Quantitative Structure-Activity Relationships, *Biopolymers 31*, 785−792.
25. Saviano, G., Crescenzi, O., Picone, D., Temussi, P., and Tancredi, T. (1999) Solution Structure of Human β-Endorphin in Helicogenic Solvents: An NMR Study, *J. Pept. Sci. 5*, 410−422.
26. Yan, C., Digate, R. J., and Guiles, R. D. (1999) NMR Studies of the Structure and Dynamics of Peptide E, an Endogenous Opioid Peptide that Binds with High Affinity to Multiple Opioid Receptor Subtypes, *Biopolymers 49*, 55−70.
27. Segawa, M., Ohno, Y., Doi, M., Ishida, T., and Iwashita, T. (1995) Solution Conformation of μ-Selective Dermorphin and δ-Selective Deltorphin-I in Phospholipid Micelles, Studied by NMR Spectroscopy and Molecular Dynamics Simulations, *Int. J. Pept. Protein Res. 46*, 37−46.
28. Tessmer, M. R., and Kallick, D. A. (1997) NMR and Structural Model of Dynorphin A (1−17) Bound to Dodecylphosphocholine Micelles, *Biochemistry 36*, 1971−1981.
29. Vold, R. R., and Prosser, R. S. (1996) Magnetically Oriented Phospholipid Bilayer Micells for Structural Studies of Polypeptides. Does the Ideal Bicelle Exist? *J. Magn. Reson., Ser. B 113*, 267−271.
30. Vold, R. R., Prosser, R. S., and Deese, A. J. (1997) Isotropic Solutions of Phospholipid Bicelles: A New Membrane Mimetic for High-Resolution NMR Studies of Polypeptides, *J. Biomol. NMR 9*, 329−335.
31. Sanders, C. R., II, and Landis, G. C. (1995) Reconstitution of Membrane Proteins into Lipid-Rich Bilayered Mixed Micelles for NMR Studies, *Biochemistry 34*, 4030−4040.
32. Chou, J. J., Kaufman, J. D., Stahl, S. J., Wingfield, P. T., and Bax, A. (2002) Micelle-Induced Curvature in a Water-Insoluble HIV-1 Env Peptide Revealed by NMR Dipolar Coupling Measurement in Stretched Polyacrylamide Gel, *J. Am. Chem. Soc. 124*, 2450−2451.
33. Glover, K. J., Whiles, J. A., Wu, G., Yu, N.-J., Deems, R., Struppe, J. O., Stark, R. E., Komives, E. A., and Vold, R. R. (2001) Structural Evaluation of Phospholipid Bicelles for Solution-State Studies of Membrane-Associated Biomolecules, *Biophys. J. 81*, 2163−2171.
34. Lindberg, M., Biverståhl, H., Gräslund, A., and Mäler, L. (2003) Structure and Positioning Comparison of Two Variants of Penetratin in Two Different Membrane Mimicking Systems by NMR, *Eur. J. Biochem. 270*, 3055−3063.
35. Andersson, A., and Mäler, L. (2002) NMR Solution Structure and Dynamics of Motilin in Isotropic Phospholipid Bicellar Solution, *J. Biomol. NMR 24*, 103−112.
36. Jeener, J., Meier, B. H., Bachmann, P., and Ernst, R. R. (1979) Investigation of Exchange Processes by Two-Dimensional NMR Spectroscopy, *J. Chem. Phys. 71*, 4546−4553.
37. Braunschweiler, L., and Ernst, R. R. (1983) Coherence Transfer by Isotropic Mixing: Application to Proton Correlation Spectroscopy, *J. Magn. Reson. 53*, 521−528.
38. Hwang, T.-L., and Shaka, A. J. (1995) Water Suppression that Works. Excitation Sculpting using Arbitrary Waveforms and Pulsed Field Gradients, *J. Magn. Reson. 112*, 275−279.
39. Piotto, M., Saudek, V., and Sklenář, V. (1992) Gradient-Tailored Excitation for Single-Quantum NMR Spectroscopy of Aqueous Solutions, *J. Biomol. NMR 2*, 661−665.
40. Mayer, M., and Meyer, B. (2001) Group Epitope Mapping by Saturation Transfer Difference NMR to Identify Segments of a Ligand in Direct Contact with a Protein Receptor, *J. Am. Chem. Soc. 123*, 6108−6117.
41. Wang, J., Schnell, J. R., and Chou, J. J. (2004) Amantadine Partition and Localization in Phospholipid Membrane: A Solution NMR Study, *Biochem. Biophys. Res. Commun. 324*, 212−217.
42. Vogel, A., Scheidt, H. A., and Huster, D. (2003) The Distribution of Lipid Attached Spin Probes in Bilayers: Application to Membrane Protein Topology, *Biophys. J. 85*, 1691−1701.
43. Bárány-Wallje, E., Andersson, A., Gräslund, A., and Mäler, L. (2004) NMR Solution Structure and Position of Transportan in Neutral Phospholipid Bicelles, *FEBS Lett. 567*, 265−269.

44. Lakowicz, J. R. (1999) *Principles of Fluorescence Spectroscopy*, Kluwer Academic Press, New York.
45. Wishart, D. S., Sykes, B. D., and Richards, F. M. (1991) Relationship between Nuclear Magnetic Resonance Chemical Shifts and Protein Secondary Structure, *J. Mol. Biol. 222*, 311−333.
46. Walsh, S. T. R., Cheng, R. P., Wright, W. W., Alonso, D. O. V., Daggett, V., Vanderkooi, J. M., and DeGrado, W. F. (2003) The hydration of amides in helices: A comprehensive picture from molecular dynamics, IR and NMR, *Protein Sci. 12*, 520−531.
47. Biverståhl, H., Andersson, A., Gräslund, A., and Mäler, L. (2004) NMR Solution Structure and Membrane Interaction Studies of the N-Terminal Sequence (1−30) of the Bovine Prion Protein, *Biochemistry 43*, 14940−14947.
48. Papadopoulos, E., Oglecka, K., Mäler, L., Jarvet, J., Wright, P. E., Dyson, H. J., and Gräslund, A. (2006) NMR Solution Structure of the Peptide Fragment 1−30, Derived from Unprocessed Mouse Doppel Protein, in DHPC Micelles, *Biochemistry 45*, 159−166.
49. Bárány-Wallje, E., Andersson, A., Gräslund, A., and Mäler, L. (2006) Dynamics of Transportan in Bicelles is Surface Charge Dependent, *J. Biomol. NMR 35*, 137−147.
50. Greenfield, N. J., and Fasman, G. D. (1969) Computed Circular Dichroism Spectra for the Evaluation of Protein Conformation, *Biochemistry 8*, 4108−4116.
51. Marinova, Z., Vukojević, V., Surcheva, S., Yakovleva, T., Cebers, G., Pasikova, N., Usynin, I., Hugonin, L., Fang, W., Hallberg, M., Hirschberg, D., Bergman, T., Langel, Ü., Hauser, K. F., Pramanik, A., Aldrich, J. V., Gräslund, A., Terenius, L., and Bakalkin, G. (2005) Translocation of Dynorphin Neuropeptides Across the Plasma Membrane. A Putative Mechanism of Signal Transmission, *J. Biol. Chem. 280*, 26360−26370.
52. Hugonin, L., Vukojevic, V., Bakalkin, G., and Gräslund, A. (2006) Membrane Leakage Induced by Dynorphins, *FEBS Lett. 580*, 3201−3205.
53. Magzoub, M., Kilk, K., Eriksson, L. E. G., Langel, Ü., and Gräslund, A. (2001) Interaction and Structure Induction of Cell-Penetrating Peptides in the Presence of Phospholipid Vesicles, *Biochim. Biophys. Acta 1512*, 77−89.
54. Uezono, T., Toraya, S., Obata, M., Nishimura, K., Tuzi, S., Saitô, H., and Naito, A. (2005) Structure and orientation of dynorphin bound to lipid bilayers by ^{13}C solid-state NMR, *J. Mol. Struct. 749*, 13−19.
55. Erne, D., Sargent, D. F., and Schwyzer, R. (1985) Preferred conformation, orientation, and accumulation of dynorphin A-(1-13)-tridecapeptide on the surface of neutral lipid membranes, *Biochemistry 24*, 4261−4263.

BI061199G